17th International Conference on Space Operations, Dubai, United Arab Emirates, 6 - 10 March 2023.

SpaceOps-2023, ID # 393

Mission Analysis of Trajectory Design and Lunar Landing on LEAD

Junji Kikuchi[a]*, Kota Tanabe[b], Masaru Koga[a], Kazuki Kariya[b], Takahiro Sasaki[b], Naoki Sato[b]

[a] *Japan Aerospace Exploration Agency (JAXA), 3-1-1 Yoshinodai, Chuo, Sagamihara, Kanagawa, Japan,252-5210*, kikuchi.junji@jaxa.jp
[b] *Japan Aerospace Exploration Agency (JAXA), 2-1-1, Sengen, Tsukuba, Ibaraki, Japan, 305-8505*
* Corresponding Author

Abstract

Aiming to realize sustainable lunar exploration, JAXA is planning to establish the Lunar Exploration Augmentation and Demonstration (LEAD) Program which will perform several technology demonstrations and science missions expecting top-level outcome worldwide. This paper reports the status of the first-phase missions for 2028 of the landing demonstration and the Lunar Navigation Satellite System (LNSS). Further, the results of the trajectory design analysis, guidance and navigation control analysis, and landing dynamics are presented. The mission feasibility is also evaluated.

Keywords: LEAD, Lunar Lander, ELFO, LNSS, Image Matching Navigation

Nomenclature

x, y, z	Body coordinate system $[m]$
X, Y, Z	Inertial coordinate system based on lunar surface $[m]$
θ	Lunar surface Inclination in inertial coordinate system$[deg]$
V_X, V_y, V_z	Initial Lander velocity in body coordinate system $[m/s]$
$\varphi_X, \varphi_Y, \varphi_Z$	Initial attitude angle in inertial coordinate system $[deg]$
$\omega_X, \omega_Y, \omega_Z$	Initial angular velocity in body coordinate system $[deg/s]$

Acronyms/Abbreviations

ELFO	Elliptical Lunar Frozen Orbit
HOI	Hohmann Orbit Insertion
IMU	Inertial Measurement Unit
JAXA	Japan Aerospace Exploration Agency
LEAD	Lunar Exploration Augmentation and Demonstration
LNSS	Lunar Navigation Satellite System
LOI	Lunar Orbit Insertion
LTO	Lunar Transfer Orbit
TCM	Trajectory Correction Maneuver
TLI	Trans-Lunar Insertion

1. Introduction

1.1 Purpose of LEAD Mission

The Japan Aerospace Exploration Agency (JAXA) proposes Japan's international space exploration scenarios (Fig.1) that outlines the next steps in the recurring lunar exploration and the technology needed to explore the Moon and Mars. [1] Aiming to realize sustainable lunar exploration, JAXA plans to establish the Lunar Exploration Augmentation and Demonstration (LEAD) Program.[2] LEAD is a lunar mission for producing scientific innovation and demonstrating advanced technology for sustainable lunar exploration, such as the Artemis mission. several technology demonstrations and science missions expecting top-level outcome worldwide. The project will provide opportunities to access missions in lunar orbit to academia and other entities. To accomplish this, a lunar lander and a demonstration satellite for Lunar Navigation Satellite System (LNSS) will be inserted to different lunar orbits after the separation from H3 launch vehicle. This paper reports the status of the first-phase missions for 2028. Further, the results of the trajectory design analysis, guidance and navigation control analysis, and landing dynamics are presented, The mission feasibility is also evaluated.

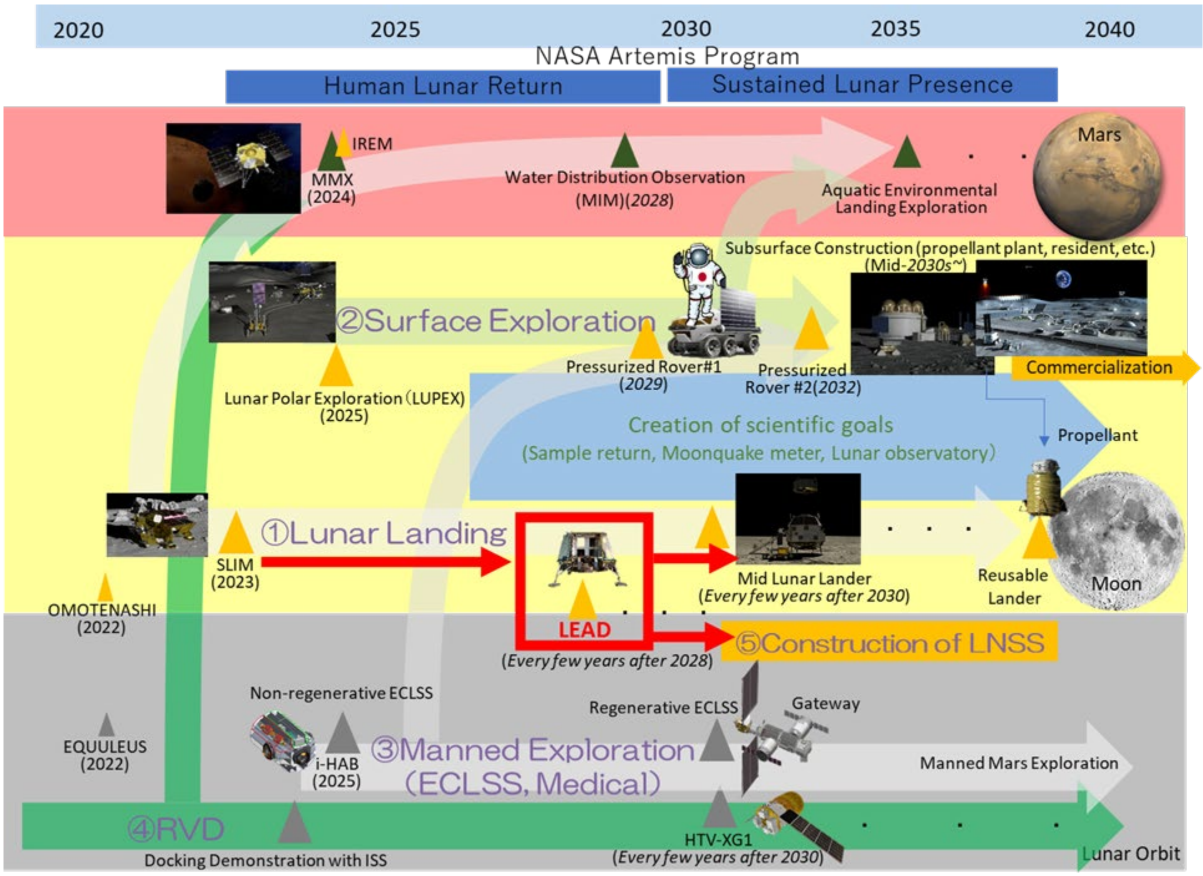

Figure 1. Japan's International Space Exploration Scenarios proposed by JAXA

1.2 Lunar Landing Mission

Currently, the target of the Artemis project is the area near the lunar South Pole where water resources are expected to be found. For lunar exploration, first-class scientific concepts are discussed at the scientific and governmental levels. Global access to the lunar surface with a flexible, highly precise landing is also expected. The goals of lunar surface missions that JAXA is considering are as follows:

- Understanding the inner structure of the Moon with the Lunar Seismograph Network.
- Selecting and collecting lunar samples, and returning them to Earth.
- Making astronomical observations from a lunar observatory on the Moon.

With the SLIM project in 2023, [3] Japan will demonstrate high-precision landing technology on mid-latitude lunar sites. Further, international space exploration scenarios by JAXA (Fig. 1) include plans for a medium-sized lunar lander to transport several tons of cargo to the Moon after 2030. However, this lander's mass and size differ from the SLIM lander. It is necessary to demonstrate the complex systems and new technologies in the LEAD mission.

1.3 Lunar Navigation Satellite System Mission

JAXA aims to provide lunar navigation services (Fig. 2) in Elliptical Lunar Frozen Orbit (ELFO) [4] to users on the lunar surface. The LNSS architecture employs several satellites orbiting the Moon that receive GNSS signals and transmit positioning data to lunar users, providing essential positioning services. As a preliminary demonstration for LEAD, a single satellite will be injected into ELFO to measure the lander's position, which has a receiver in the South Polar region.

Positional accuracy is affected by ranging and spatial propagation delay errors caused by inaccurate estimates of a satellite's orbital period and the orbital environment. Further, since the effect of the lunar surface environment on the LNSS signal can be measured accurately, it is essential to conduct a demonstration before establishing the constellation infrastructure. There are currently no international projects to generate and transmit positioning signals from lunar orbit to the surface. A demonstration of this system will establish the basic technology to support navigation necessary for lunar exploration.

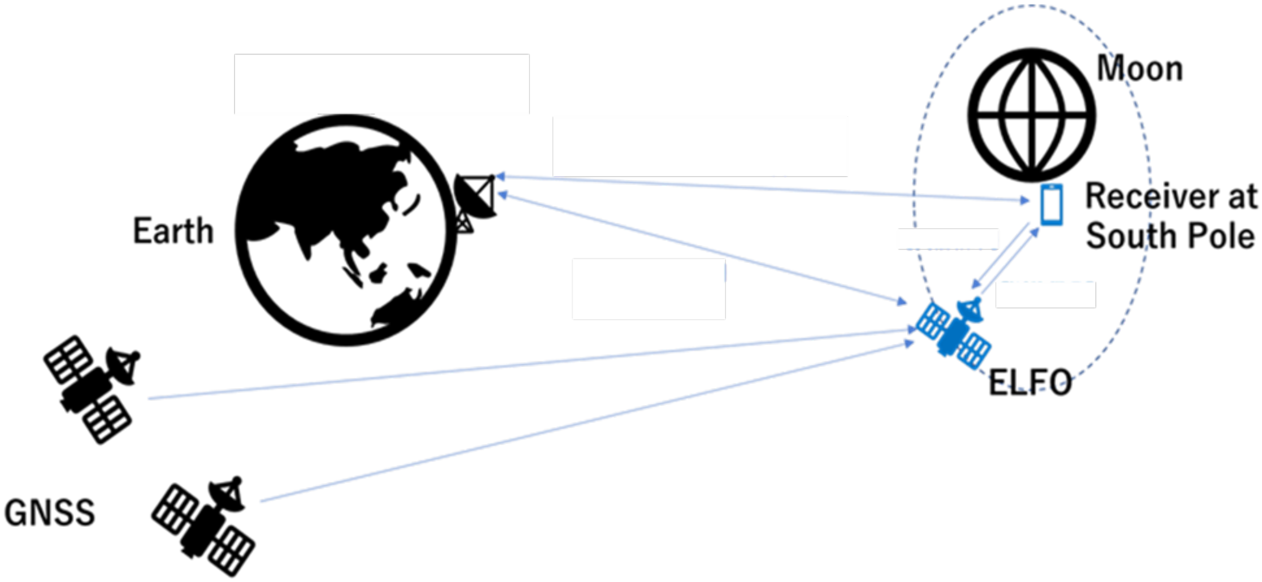

Figure.2 Lunar Navigation Satellite System (LNSS)

2. Trajectory Design

2.1 Trajectory Overview

The trajectory design of the two LEAD spacecraft is shown in Fig. 3. The spacecraft are launched by H3 rockets and inserted into an elliptical Earth orbit with an apogee altitude of 230000 km. The lander then performs a Trans-Lunar Insertion (TLI) at the perigee to inject the spacecraft into a Lunar Transfer Orbit (LTO). The lander separates from the LNSS satellite, and the two spacecrafts transfer into different orbits.

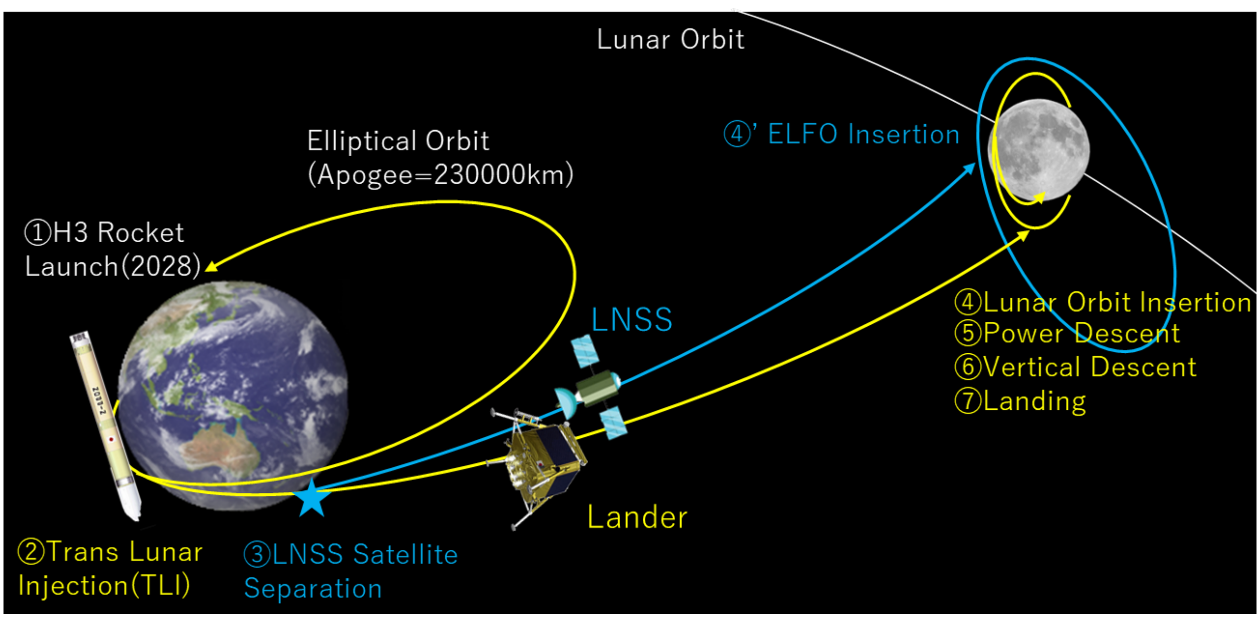

Figure.3 Trajectory Overview of LEAD mission

2.2 Landing Trajectory Design

This section describes the trajectory planning method for the lander. First, the landing site of the lander must be evaluated to determine the launch timing. The landing site must have an established communication path to the ground station and be in daylight. In particular, since the lander will be landing in the Antarctic region, the sun angle will be very low, generating significant constraints on the timing of image navigation. In this analysis, CR1 in the Antarctic region is set as a tentative target site, and the communication path and solar angle are evaluated within 2028.

Figure 4 shows the visibility of the Uchinoura ground station in Japan, and the solar angle at the landing site in 2028. In particular, the solar angle is a maximum in October. The red frame in Figure 4 indicates the areas where visible time is available and the solar angle is above 0º. The landing date selected was October 5, 2028, when the highest solar angle in this area will occur.

Table 1. Lunar Coordinates of CR1

Landing Site	Latitude	Longitude	Radius
CR1	-89.439[deg]	-137.134[deg]	1739.3[km]

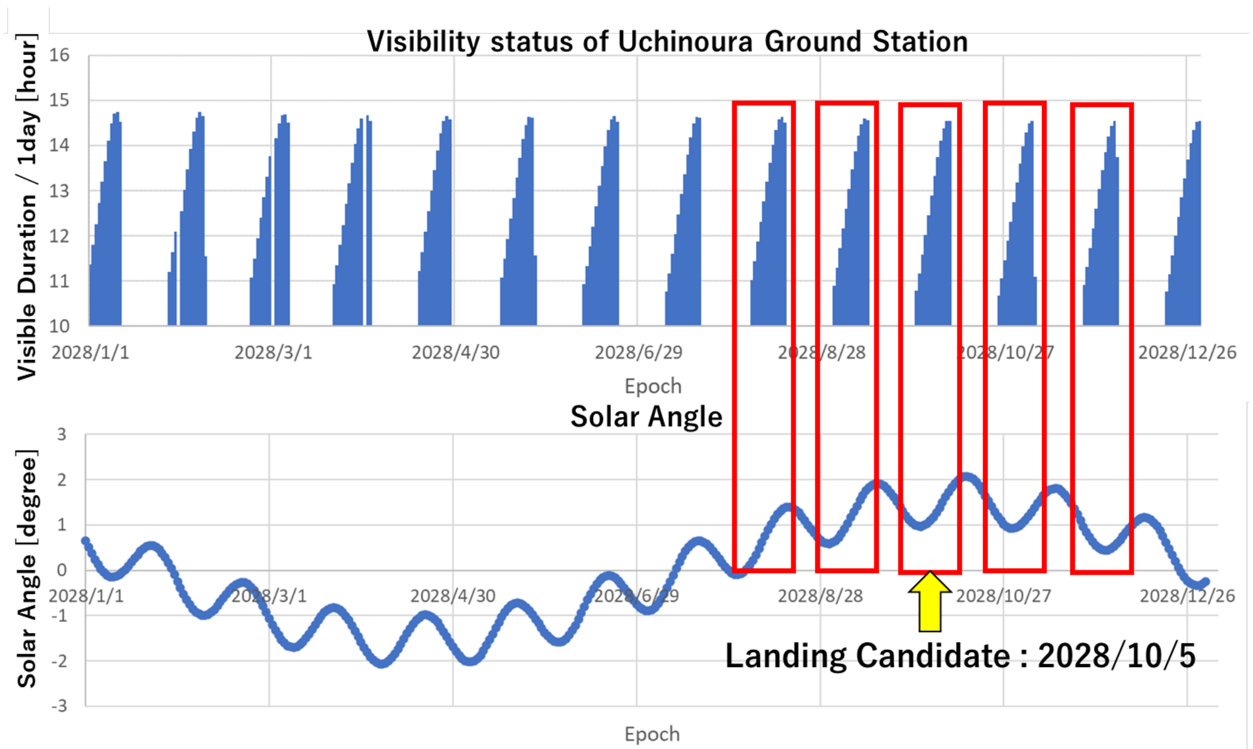

Figure.4 Landing Site Evaluation (Up : Visibility of Uchinoura ground station in Japan, Below: solar angle)

The landing point as shown in Table.1 is set as the target, and trajectory is planned by a back propagation. After the TLI at the perigee of an elliptical Earth orbit, the lander reaches the vicinity of the Moon and enters a polar orbit with an inclination of 90º by LOI. A polar orbit provides access to the entire lunar surface. The LOI is not performed once but is divided into three times to transfer to the 100 km circular orbit. A single, large LOI would make it difficult to correct the orbit due to attitude control and thrust errors. As shown in Figure 5, the LOI is divided into three times: 100x8700 km after the first LOI, 100x1400 km after the second LOI, and the third LOI that enters the 100 km circular orbit. The 100 km orbit is used as a parking orbit before transitioning to landing. This reduces the amount of ΔV required for the landing and allows for more accurate observation of the lunar surface conditions. On the other hand, the orbit will be affected by the solar power generation cycle due to the Moon's shadow and a disturbance caused by the stronger lunar gravity. Further, by entering a circular orbit instead of an elliptical one, the timing of the maneuver for the landing can be determined regardless of the orbital phase. Then, it makes a Hohmann transition to an altitude of 15 km and begins a powered descent. The ΔV budget for the lander is shown in Table 2. The total TCM was estimated to be 5% by a Monte Carlo analysis that considered the lander's rocket guidance, attitude control, and thrust errors.

2.3 LNSS Trajectory Design

The LNSS satellite will be injected into a stable ELFO for a positioning demonstration. This ELFO minimizes the control required to maintain orbit, saving fuel and providing stable positioning. The ELFO inclines of 56.2º, and other orbital elements are also fixed as shown in Table 2. This inclination is significantly different from the lander, so the LNSS satellite must reach ELFO independently. Therefore, the lander performing the LNSS satellite separates immediately near the Earth after the TLI. After separation from the lander, the orbit determination of the LNSS satellite is conducted for a day, at which point the trajectory is designed by forward propagation. If the orbit control is not performed, the LNSS satellite will enter the same polar orbit as the lander, so TCM is performed after the orbit determination and the LNSS satellite is injected into the ELFO transfer orbit. Since the departure point and the orbital parameters of ELFO are fixed. The only free variables are the true anomaly and the RAAN when injected into ELFO. The LOI is not divided, and the satellite is injected into ELFO in a maneuver (Fig. 6). This is because dividing the LOI complicates the correction of each orbital element of the ELFO.

The ΔV budget for the lander and the LNSS satellite is shown in Table 3. The total TCM is estimated to be 5% from a Monte Carlo analysis that takes into account rocket guidance error, attitude control error, and thrust error of the lander.

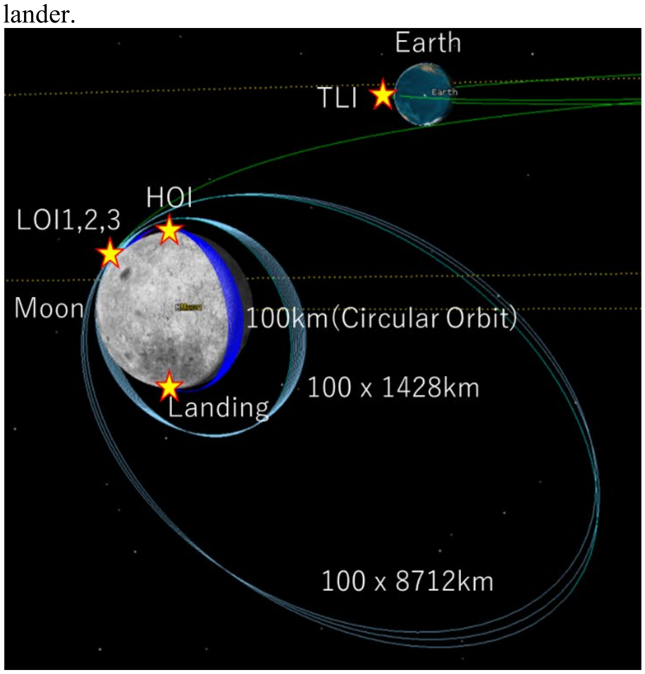

Figure.5 Trajectory Design of Lander mission

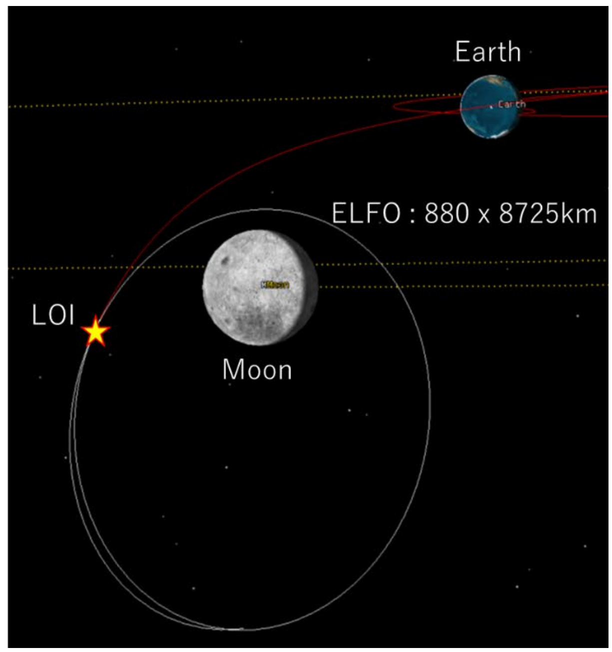

Figure.6 Trajectory Design of LNSS mission

Table 2. Orbit Parameters of ELFO

Parameter	Semimajor-Axis	Eccentricity	Inclination	Argument of Perigee	RAAN	True Anomaly
Value	6541.4[km]	0.6	56.2[deg]	90.0[deg]	Variable	Variable

Table 3. Sequence of events and ΔV[m/s] Summary

No	Sequence	Lander	LNSS Satellite
1	H3 Rocket Launch	-	-
2	TLI	63.6	-
3	LNSS Satellite Separation	-	-
4	LOI1	294.5	
5	LOI2	292.9	483.7
6	LOI3	203.8	
7	HOI	19.7	-
	Total TCM (5%)	43.7	24.2
	Sum	918.2	507.9

3. Guidance and Navigation Analysis

Once the lander reaches an altitude of 15 km, the powered descent phase is started (Fig.7) with a deceleration boost. The powered descent will end at an altitude of 4 km above the landing site, with zero vertical and horizontal velocity at that point. The effect of navigation errors caused by the Inertial Measurement Unit (IMU) is large, and a method that allows on-line recalculation of trajectory is required for accurate landings. Therefore, the lander must perform surface-based onboard navigation to determine its position with respect to the lunar crater, so the lander resets the navigation error to achieve a highly accurate landing. Moreover, a guidance law with a low computational cost would be indispensable to reflect the observed position and velocity data obtained from image matching. The lander uses the polynomial guidance law developed for SLIM to generate a nominal trajectory. The polynomial law is computationally inexpensive, and trajectories can be recomputed online, allowing data from image matching to be reflected in the next boosting phase. The onboard navigation is performed three times during the powered descent.

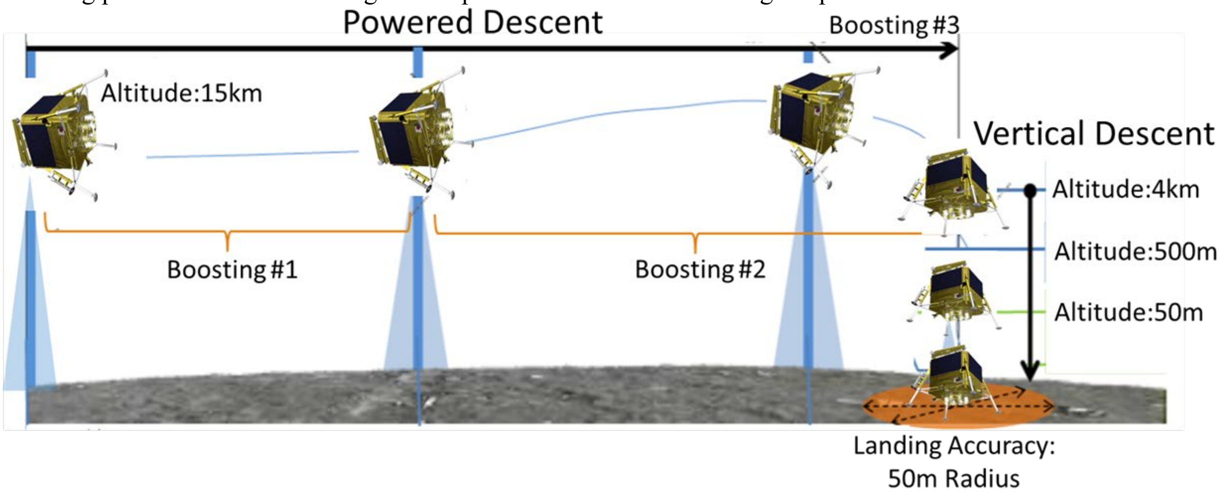

Figure.7 Powered and Vertical Descent

Table 4 shows the design parameters for the powered descent analysis. The IMU for the lander is tentatively chosen to be Northrop Grumman's LR-450. RCS performs attitude control. During image navigation, the lander will coast for 50 seconds to improve measurement accuracy, during which the main engine will be turned off. The accuracy of the image navigation depends on the altitude position at that time, and the accuracy improves when the observation is closer to the lunar surface. The minimum altitude for image navigation is 4 km.

The figure shows the downrange and the lunar altitude of the nominal trajectory of the powered descent analysis. The lunar surface is assumed to have a uniform radius of 1738 km. By implementing each error parameter in the Monte Carlo analysis, the horizontal end positional accuracy is expected to be about 100 m(3σ).

Table 4. Analysis Parameter of Powered Descent

Parameter	Design Value
Mass	3.254[ton]
Moment of Inertia	(Ixx, Iyy, Izz) = (5402, 5402, 5657) [$kg \cdot mm^2$]
Engine Thrust	6.0[kN]
RCS Torque	288.96[Nm]
Image Navigation Accuracy	Altitude : 50.0m per 1km(3σ) Horizontal : 5.2m per 1km(3σ)

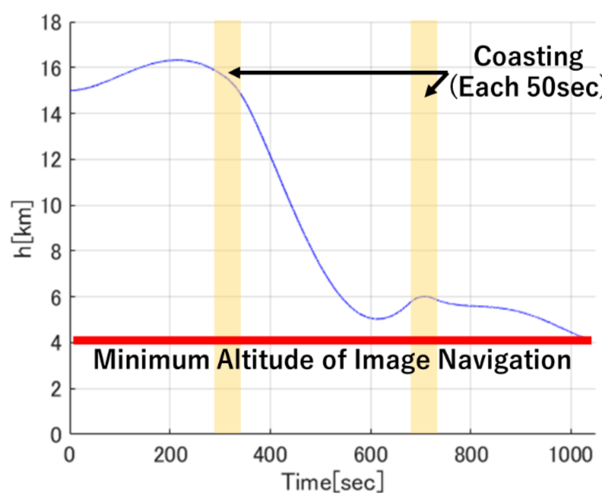

Figure.8 Nominal Trajectory of Powered Descent

Vertical descent begins at an altitude of 4 km. This is decided by constraints imposed by the radar detection range. The horizontal positioning accuracy at the end of the powered descent is the distance that must be corrected in the vertical descent. The goal is to be within 50 m of the target by the touchdown. During the descent, the lander detects obstacles and craters on the surface and avoids them. The lander approaches the Moon within 3 m and then begins free fall. Doctor Sasaki et al. are analyzing the vertical descent and studying control methods to keep the landing accuracy within 50 meters. [5] The analysis is expected to result in a table of residual errors at a lunar altitude of 3 m, which is the terminal point of the vertical descent. Table 5 summarizes the ΔV for the powered and vertical descent. This ΔV value varies greatly depending on the thrust power.

Table 5. ΔV Summary of Landing Phase

Phase	Powered Descent	Vertical Descent
ΔV	2007.9	392.0

3. Landing Dynamics Analysis

After free fall from 3 meters, the landing must be successful with a high probability. Landing stability is a significant issue, and an effective lander leg design is essential. This study evaluated a leg system (Fig.9) consisting of a combination of main and secondary legs with built-in crushable materials as referring to the developed example of the Martian Moons eXploration (MMX) mission of JAXA is evaluated.[6] Table.6 shows the lander size and mass model. The design parameters include leg width, attachment angle, and pad diameter. Moreover, the crushable material has its parameters such as plateau stress and stiffness. Numerical integration simulations were run using ADAMS, a general-purpose solver. Because errors also occur at the end of vertical descent (e.g., in the lander's position, velocity, attitude, and angular velocity), these were included in the Monte Carlo analysis to evaluate their effects as shown in Table 8.

A ground model as shown in Fig.10 is reproduced for analyzing the condition of the lunar surface, based on NASA lunar observation data, paying attention to obstacles and craters. [7] [8] This allows the simulation to reproduce tipping due to leg trapping. Parameters such as the stiffness and friction rate of the lunar surface are shown in Table 7 for the conditions used in previous SLIM and SELENE-B analyses.[9][10] It is also expected that the surface will be inclined. The Monte Carlo analysis assumed the lander would be on an incline of 15º or less to the lunar surface.

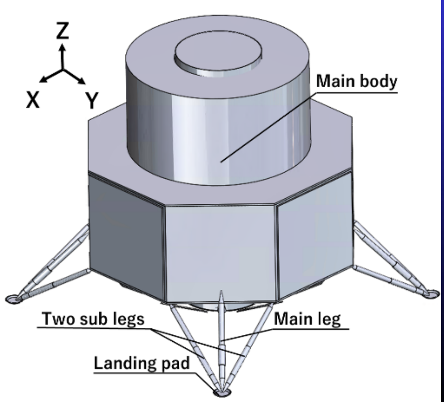

Figure 9. Landing Leg System

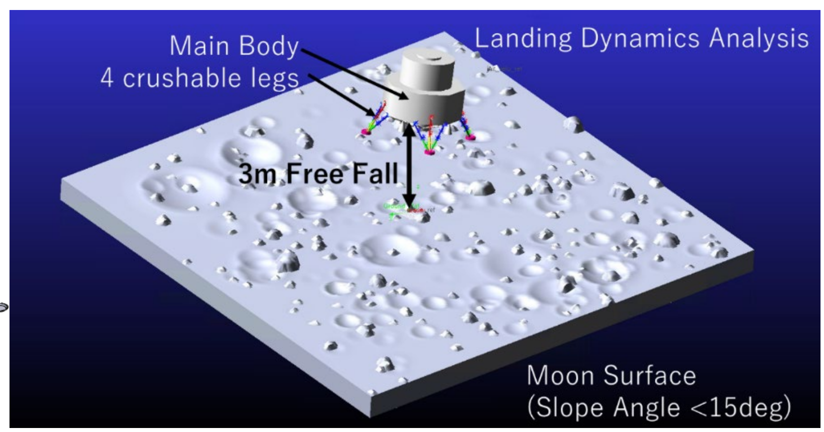

Figure 10. Landing Leg System

Table 6. Analysis Model of Lander and Landing leg

Parameter	Design Value
Mass	1350$[kg]$
Size	Width = 3.25$[m]$, Height = 4.65$[m]$ Octagonal shape without legs
Center of Mass	(x, y, z) = (0.00, 0.00, 1.00) $[m]$ without legs
Moment of Inertia	(Ixx, Iyy, Izz) = (301.95, 301.95, 331.57) $[kg \cdot mm^2]$
Landing Leg	Length = 1352[mm], Leg Opening Angle = 73[degree]

Table 7. Lunar Surface Parameter

Parameter	Value
Coefficient of Restitution	$10[N/mm]$
Index of Restitution	1.3
Maximum Damping Coefficient	$20[N \cdot s/mm]$
Penetration Depth	$0.5[mm]$
Coefficient of Friction	0.8

Table 8. Initial Conditions of Monte Carlo Analysis

Parameter	Variable Value
Inclination Angle	0, 3, 6, 9, 12, 15 [degree]
Vertical Position	$Z = 3.000 \pm 0.300[m](3\sigma)$
Horizontal Position	$X, Y = \text{Random}$
Velocity	$V_X, V_y = \pm 0.025[m/s](3\sigma)$ $V_z = \pm 0.800[m/s](3\sigma)$
Attitude	$\varphi_X, \varphi_y = \pm 0.300[deg](3\sigma)$, $\varphi_z = Random$
Angular Velocity	$\omega_X, \omega_y, \omega_z = \pm 0.020[deg/s](3\sigma)$

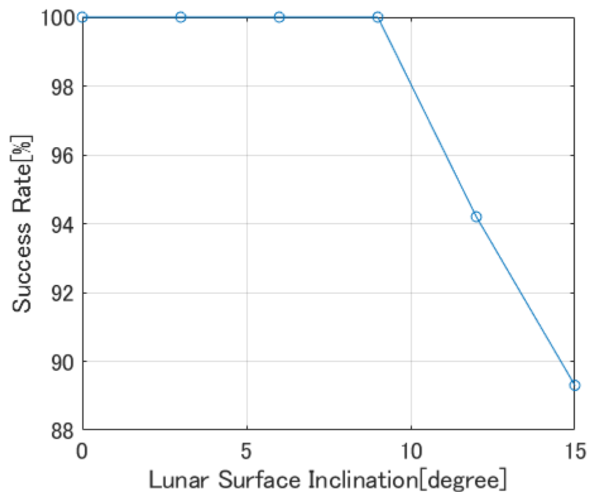

Figure 11. Success Rate of Landing vs Inclination Angle

Figure 12 shows the probability of a successful landing for various inclinations. The failure case is determined when the lander's axis is inclined 80 º or more relative to the ground angle. These results indicate that when the ground angle is less than 9 º, the success rate of the landing is 100%. On the other hand, the success rate decreases when the ground angle is 12 º or more. From the bounce until the lander stabilized, there were many cases in which the pad interfered with obstacles on the lunar surface and tipped over. LEAD has set a target landing success rate of 3σ (=99.73%) or higher. Based on this analysis, the following measures should be taken

- Set a lower maximum ground angle.
- Increase the leg opening angle by adopting folding legs and other measures.
- Lowering the center of gravity position.

Conclusion

In an effort to realize a sustainable lunar exploration future, this paper provides an overview of the Lunar Exploration Augmentation and Demonstration (LEAD) program and the latest study status. The methods of trajectory design, guidance and navigation control, and landing dynamics analysis are described. Based on the results of ΔV and landing success rate, studies on the capabilities required for the system and the various constraints from launch to operation are underway. We will continue to study these and other factors for the early launch of LEAD to play a leading role in creating world-class scientific results and developing fundamental technologies and commerce necessary for lunar exploration.

References

[1] Kathleen C. Laurini, Bernhard Hufenbach, Juergen Hill, and Alain Ouellet.: "The Global Exploration Roadmap and Expanding Human/Robotic Exploration Mission Collaboration Opportunities," IAF 66th International Astronautical Congress, October 2015, A3.1.1
[2] Kota Tanabe, et al. "Plan Overview of Lunar Exploration Augmentation and Demonstration (LEAD)", 4F02 (in Japanese)
[3] Tetsuhito Arakawa, et al. "System of Small Lunar Lander", Proceedings of the Space Sciences and Technology Conference, 2018, ID02 (in Japanese)
[4] Todd A.Ely, et al. "Constellations of EllipticalInclined Lunar Orbits Providing Polar and Global Coverage", AAS/AIAA Astrodynamics Specialists Conference, August 2005, AAS 05-343
[5] Takahiro Sasaki, et al. "Vertical Descent Guidance and Sequence Optimization for Lunar Landing Mission", 32nd Workshop on JAXA Astrodynamics and Flight mechanics, 2022

[6] Masatsugu Otsuki, et al. "Subsystem Development of the Martian Moons Exploration (MMX) (Landing Gear: In-House Study)", 2022, 2D11 (in Japanese)
[7] Roberts Barry C，Cross-Program Design Specification For Natural Environments (Dsne) Revision G，https://ntrs.nasa.gov/citations/20200000867
[8] Kazuki Kariya, et al. "High-Resolution Lunar Terrain Modeling for Evaluating Hazard Detection and Avoidance", Proceedings of the Space Sciences and Technology Conference, 2018, 1D13.
[9] Taro Kawano, et al. "Study of Leg Arrangement for Stable Touchdown during Two-step Landing for SLIM", AEROSPACE TECHNOLOGY JAPAN, 2020, Vol. 18, No. 5, p. 222-230
[10] Masahiro Nohmi, et al. "Contact Dynamics Analysis and Stability Evaluation for Lunar Lander with 4 Legs", Transactions of the JSME (Version C), 2012, Vol 78, No. 790, p.-1960-1971(in Japanese)